Title
COLLISIONLESS NON-RADIATIVE DECAY RATES OF SINGLE ROTATIONAL LEVELS OF S1 FORMALDEHYDE

Author
Weisshaar, J.C.

Publication Date
1979-02-01

Submitted to the Journal of Chemical Physics

Preprint

COLLISIONLESS NON-RADIATIVE DECAY RATES OF SINGLE ROTATIONAL LEVELS OF S_1 FORMALDEHYDE

James C. Weisshaar and C. Bradley Moore

February 1979

Prepared for the U. S. Department of Energy
under Contract W-7405-ENG-48

Collisionless non-radiative decay rates of single rotational levels of S_1 formaldehyde

James C. Weisshaar and C. Bradley Moore
Department of Chemistry, University of California, Berkeley, California 94720
and
Materials and Molecular Research Division
of the
Lawrence Berkeley Laboratory, Berkeley, California 94720

Fluorescence lifetimes of single rotational levels of the lowest vibrational level of the first excited singlet state of H_2CO and D_2CO have been measured under collision free conditions following excitation by a pulsed dye laser. For H_2CO, the lifetimes range from 66 ns to 4.2 μs with a median of about 160 ns. Individual lifetimes show no systematic variation with J', K', or E_{rot}. K-doublet levels split by as little as 8×10^{-4} cm^{-1} in S_1 are observed to have different lifetimes. The H_2CO results are interpreted in terms of a sequential coupling model ($S_1 \rightarrow S_0 \rightarrow$ continuum) in which the final states are those of the H_2 + CO dissociation continuum. For D_2CO, the lifetimes vary between 5.8 and 8.1 μs and are nearly radiative lifetimes.

I. INTRODUCTION

Until very recently, non-radiative decay rates of polyatomic molecules have been studied only to the level of detail of initially prepared single vibronic levels.[1] Very little is known about the decay of single rotational states. Theoretical treatments have usually considered only vibronic intramolecular perturbations; the rotational degrees of freedom have been ignored.[2] Experimental work has been limited by laser linewidths, by poor signals at pressures for which rotational relaxation is unimportant, and by the high density of rovibronic transitions for larger molecules. The availability of better lasers and the possibility of cooling large molecules in a nozzle expansion[3] improves the experimental situation.

There are only a handful of studies concerned with the fate of single rovibronic levels. Rotational relaxation is very fast and converts an initial state to a broad distribution of other S_1 states in the cases of glyoxal[4, 5] and benzene.[6] Naphthalene[7] and formaldehyde[8 - 11] have been shown to exhibit a partially resolved rotational state dependence of fluorescence quantum yield and S_1 lifetime. Such effects were searched for, but not observed, in glyoxal[5] and benzene.[12] Rapid rotational relaxation may render studies of the rotational state dependence of electronic quenching impossible. It is increasingly clear that "zero pressure" may occur at lower pressures than was previously expected.[6, 10]

This paper reports direct measurements of the fluorescence decay rates of single rotational states of S_1 formaldehyde at pressures low enough to preclude significant collisional relaxation. The H_2CO lifetimes for the 4^0 level vary by more than a factor of 50 with rotational state. The results suggest possibilities for the photochemical decay mechanism of formaldehyde as well as for the role of rotational state in the nonradiative decay of intermediate-sized molecules.

II. EXPERIMENTAL

Many of the experimental details have already been described.[10] Only the relevant modifications and additions will be discussed here. Pressures near 1 mtorr were measured to better than ± 20% with a 0 - 1 torr capacitance manometer (Baratron 310-BH) connected directly to the fluorescence cell. For these higher resolution studies, the N_2 laser pumped dye laser included an air-gap etalon (2 cm^{-1} FSR, nominal finesse of 25) in the oscillator. Both the etalon and the grating were contained in a pressure tank which provided smooth wavelength tuning when pressurized with N_2 gas through a needle valve. A typical laser output energy near 370 nm was 0.1 mJ per pulse using the dye BPBD in 2:1 ethanol/toluene. Shot-to-shot fluctuations in the pulse energy and in the fluorescence intensity were about 10%, indicating good frequency stability. The oscillator lased on a single etalon mode, as evidenced by the extinction of the output between modes as the etalon was tilted, and by the absence of 2 cm^{-1} periodicity in the excitation spectra described below.

The laser pulses passed through two separate fluorescence cells, each equipped with an RCA 8575 photomultiplier tube for viewing fluorescence perpendicular to the beam. One cell, described previously,[10] was equipped with four baffles made of red glass cutoff filters and supported by glass sleeves. This cell was used to obtain fluorescence decay curves for low pressures of formaldehyde. Two cm of nearly saturated solution of $NaNO_2$ in water was used between the viewing window and the PMT as a uv cutoff filter. The filter transmits > 60% above 430 nm and < 0.5% below 410 nm.

A second fluorescence cell was a 20 cm long, 2.5 cm i.d. quartz cylinder used to obtain fluorescence excitation spectra of formaldehyde at pressures in the range 1 to 5 torr. A glass uv cutoff filter (50% T at 408 nm) was used between the cell and the PMT to diminish scattered light. Current pulses from the second PMT were fed to a gated electrometer whose time aperture was set to integrate the entire fluorescence pulse. The electrometer output voltage was applied to the Y input of an analog XY plotter whose X axis followed the output voltage of a capacitance manometer (Validyne DP-7, 20 psi diaphragm) connected to the pressure tank of the dye laser. In this way, the X axis was linear in the tank pressure, and hence the wavelength, independent of the time linearity of the pressure. The spectrum of total fluorescence intensity vs wavelength was obtained in 10 cm^{-1} intervals, corresponding to pressure scans of ~ 20 psi of N_2. After each scan, the grating was manually tilted to set the initial wavelength for the next scan.

A segment of the 4_1^0 spectrum of H_2CO is shown in Fig. 1. The FWHM of the laser, as estimated by the width of the well-isolated features, is 0.15 cm^{-1} for this scan. The linewidth varied between 0.10 and 0.25 cm^{-1} from time to time, with 0.15 cm^{-1} quite usual. Such linewidths are broader than the Doppler width of 0.06 cm^{-1} but are sufficiently narrow to excite single rotational levels quite selectively in many cases.

After a 10 cm^{-1} spectrum had been recorded, a particular absorption feature could be excited by pressure tuning to the wavelength of interest. The first fluorescence cell was filled with a low pressure of H_2CO and a decay curve was obtained by averaging ~ 1000 shots of fluorescence plus scattered light, pumping out the cell, averaging the same number of shots of scattered light, and digitally subtracting the two curves. This process required about 15 min. Once set, the laser wavelength was stable for an hour or longer, as monitored by changes in the average fluorescence signal from the second cell.

The t = 0 amplitude of the scattered light pulse was as much as 100 times that of the fluorescence signal for the weakest absorption features studied at mtorr pressures. For lifetimes faster than ~ 200 nsec, the PMT current passed through a 50 Ω load and the 1/e fall time of the scattered light pulse was 7 nsec. In these cases, the first 50 nsec or so of the fluorescence decay was obscured by scattered light and was discarded. Decay components faster than ~ 25 nsec would not have been observed unless they were very strong. Longer time constants were used for longer lifetimes. The 1/e fall time of the scattered light was always at least eight times shorter than the lifetime being measured.

For the single exponential decays, the log plots of fluorescence intensity vs time were typically linear over 1.5 decades. The decay times are considered accurate to within ± 5%. They are typically reproducible to within ± 5% from day to day. The few non-exponential decays reported were fit as a sum of two exponential decays with rates whose accuracy is typically ± 15%. In some cases the slow component was very weak and was determined to only ± 50%. The $t = 0$ relative amplitude of the two components, I_f/I_s, is accurate to ± 30%.

III. RESULTS

A. Spectroscopy

The rotational structure of the 4_1^0 hot band absorption of H_2CO has been nearly completely assigned by Sethuraman, Job and Innes.[13] For D_2CO, the assignments used were those of Orr.[14] It was a relatively easy matter to calibrate the wavelength scale of an excitation spectrum and match numerical assignments with observed fluorescence peaks. With only two exceptions out of about 200 cases,[15] every assigned wave-number value matched an observed peak within the present resolution of ± 0.1 cm^{-1}. Additional unassigned lines were quite common, especially near the band center. These were almost always weak and can be attributed mainly to $K' = 0$ and 2 lines, none of which have been assigned.

The 4_1^0 band is perpendicular[16] (type B), and primarily rR and rQ lines were studied, since they are strong and lie on the relatively uncongested blue side of the band. (The notation $rQ_{K''}(J'')$ denotes a $\Delta K = + 1$, $\Delta J = 0$ transition in absorption from the $J''K''$ ground state). In both the upper and lower states of the 4_1^0 transition, H_2CO is a slightly asymmetric, near-prolate top[13] ($\kappa = -0.9699$ for 4^0 and $\kappa = -0.9675$ for 4_1). The usual practice is to classify rotational states under the symmetry operations of D_2, the rotational sub-group for the asymmetric top, rigid rotor Hamiltonian.[17] The operations are $C_2{}^a$, $C_2{}^b$, and $C_2{}^c$, which are rotations about the (molecule-fixed) principal inertial axes a, b, and c. Each state is symmetric (+) or antisymmetric (-) with respect to these operations, and specification of any two symmetries determines the third. The notation (+-), (--), etc. gives the behavior under C_2^c (first label) and C_2^a (second label). In this paper, K refers to the good quantum number K_{-1} in the prolate top limit; the C_2^a label is + or - for K even or odd. Similarly, the parity of the oblate top limit quantum number K_1 corresponds to the sign of the C_2^c label, so that the $J_{K_{-1}K_1}$ notation[18] is easily related to the (+-) notation.

A more rigorous technique which does not rely on the separation of electronic, vibrational, and rotational coordinates involves classifying each zeroth-order wavefunction under the full symmetry group of the Hamiltonian,[19] which is isomorphic with C_{2v}. This permits definitive statements as to which levels can or cannot be coupled by intramolecular perturbations. For C_{2v} symmetry (as in S_0), each of the four rigid rotor D_2 species has a different representation under C_{2v} as follows: (++) $\rightarrow$ ${}^rA_1$, (-+) $\rightarrow$ ${}^rA_2$, (--) $\rightarrow$ ${}^rB_1$, (+-) $\rightarrow$ ${}^rB_2$. For C_s symmetry (as in non-planar S_1), the correspondence is : (++) and (--) $\rightarrow$ ${}^rA'$; (-+) and (+-) $\rightarrow$ ${}^rA''$. The overall rovibronic species is obtained in the usual way by taking the direct product of the electronic, vibrational and rotational species.

The splitting of the K-doublets due to asymmetry increases with J but decreases rapidly with K. In either electronic state, for thermally important transitions, the splitting is smaller than the Doppler width (0.06 cm^{-1}) for $K \geq 3$, so that S_1 doublet components cannot be selectively excited for $K' \geq 4$. In these unresolved cases, the laser populates both doublet components equally. For $K' \leq 3$ the doublets are typically resolved and assigned, so that a particular component can be excited. An example is the case of rQ_2 excitation. The $K' = 2$ doublet becomes resolvable for $J' \geq 6$ and two lines are observed. Because of the selection rule, for $K' = 3$, $J' \geq 6$ it is possible to excite either the (+-) or (--) component even though they are split by as little as 8×10^{-4} cm^{-1} in S_1.

The purity of excitation of a particular rovibronic transition is difficult to assess, since weak unassigned transitions could always overlap the desired transition within the laser linewidth. Features that were obviously broader than the laser or that showed poorly resolved shoulders were avoided. Assigned features within 0.2 cm^{-1} of each other were not well resolved. Results are reported only for cases of apparently clean excitation.

B. Pressure dependence of fluorescence decays

The total fluorescence after apparently clean excitation of a particular S_1 rotational level at low enough pressure nearly always decays as a single exponential, and the decay rate varies more than a factor of 50. At higher pressures, there is competition among rotational relaxation within 4^0, vibrational relaxation to 4^1, and electronic relaxation out of S_1. Since total fluorescence is observed, relaxation to states of primarily longer lifetime should appear as a long-lived tail on the main decay.

Only a few Stern-Volmer plots were generated. Several distinct types of behavior were observed. For long-lived states having τ_0 = 450 ns to 4.2 μs, the decays are single exponentials and the Stern-Volmer plots are linear from about 0.5 to 10 mtorr. The quenching rates are typically ~ 100 μs^{-1} $torr^{-1}$, or about 10 gas kinetic. Examples include $rR_0(2)$, $rQ_0(4)$, $rQ_0(6)$, and $rQ_0(7)$. For faster decaying states, a slower tail grows in with pressure, typically above 5 mtorr, indicating that rotational/vibrational relaxation within S_1 at least competes with electronic quenching. Examples include $rR_6(9)$ (τ_0 = 88 nsec) and $rQ_0(5)$ (τ_0 = 298 nsec). For $rQ_0(9)$ (τ_0 = 313 nsec), the decays became slightly non-exponential above a few mtorr, but a resolution into fast and slow components was impossible. Finally, for the rapidly decaying state $rR_6(9)$ (τ_0 = 88 ns), a plot of inverse relative fluorescence quantum yield, ϕ_f^{-1}, vs pressure was obtained by integrating the fluorescence intensity vs time curves and normalizing the area to the peak intensity. ϕ_f increased very slightly (by less than 10%) between 10^{-3} and 0.1 torr, presumably reflecting a competition between electronic relaxation and rotational relaxation to longer-lived states.

For each rotational state, it was desirable to measure only a single decay time at a pressure low enough so that collisions caused a small deviation from the true zero pressure lifetime τ_0. Based on the Stern-Volmer plots mentioned above and on quenching results from previous broadband work,[10] 200 μs^{-1} $torr^{-1}$ is an upper limit for the total relaxation rate out of a single rotational level of 4^0 H_2CO. Thus it can be estimated, for example, that a measured lifetime of 200 ns at 10^{-3} torr has been collisionally shortened by less than 4%. In all but one case ($rR_2(13)$, (--)) listed in Table I, the estimated deviation from τ_0 is less than 10%, and in most cases it is 2 - 5%. For the few lifetimes longer than 1 μs, Stern-Volmer plots were generated and zero pressure extrapolations were performed to obtain the τ_0 listed in Table I. In general, systematic underestimation of τ_0 due to collisional effects at finite pressures is comparable to the accuracy of the lifetimes themselves, about 5%.

C. Zero pressure exponential decays

H_2CO results. For the 4^0_1 band of H_2CO, in over 90% of the cases of apparently pure excitation at low enough pressure the decay of fluorescence was a single exponential over 1.5 decades. Two typical decays are shown in Fig. 2. The lifetimes, pressures, and rigid rotor energies are given in Table I for the 104 cases of single exponential decay. The upper state quantum numbers range from $K' = 1$ to 11 and $J' = 3$

to 22. No assignments were available for $K' = 0$ and 2 lines. The completeness of coverage of quantum numbers was limited by absorption intensities and spectral overlaps.

In one case, that of $rQ_2(6)$ excitation, the two K-doublet lines were only partially resolved since their spectroscopic splitting is only 0.16 cm^{-1}. By tuning the laser to either edge of the doublet, it was possible to excite primarily either the (+-) or (--) component. In either case, a biexponential decay was observed with the same two lifetimes; however, the relative $t = 0$ amplitude changed a factor of seven as the laser frequency was changed. The assignment of the lifetimes to the individual components was thus clear, and the two components are included in Table I.

In favorable cases it was possible to cleanly excite the same upper state via two different transitions, e.g., both $rR_8(15)$ and $rQ_8(16)$ terminate on $J' = 16$, $K' = 9$. Such cases provide a cross-check on the rotational assignments as well as the lifetimes and excitation selectivity. Fourteen such cases were checked, and in all fourteen the lifetimes agreed quite satisfactorily. The average deviation of the two lifetimes from their mean was 4%, confirming the estimated accuracy of the lifetime measurements.

The single exponential lifetimes range from 66 ns to 4.17 μs, but lifetimes shorter than 100 ns or longer than 500 ns are unusual. Figure 3 shows a bar graph of frequency of occurrence of decay rate over 1 μs^{-1} intervals. The mean decay rate of the 90 different states represented in Table I is 6.2 μs^{-1}, so a representative lifetime is about 160 ns.

Trends of τ_0^{-1} with J' or K' are not obvious. Figure 4 shows a detailed plot of the rates vs J' for various K'. For a given K', there is no apparent trend with J', nor is there a systematic difference between (+-) and (--) states. Similarly, for a given J', there is no systematic variation of rate with K'. However, on the average, τ_0^{-1} tends to increase with either K' or the S_1 rotational energy E_{rot}. The rates averaged over J' for a particular K' are shown in Fig. 5. The increase in mean τ_0^{-1} with K' is about a factor of three as K' increases from 1 to 6. There is no evidence that even and odd K' states behave differently. The analogous plot of rates averaged over K' for each J' shows no trend. The average rate over 100 cm^{-1} intervals of E_{rot} shows an increase with E_{rot} very similar to that with K'. (These variables are highly correlated, since the K^2 term dominates the J^2 term in E_{rot}). Note that lifetimes longer than 500 ns were not observed for $K' > 4$ or for $E_{rot} > 300$ cm^{-1}.

D_2CO results. For 4_1^0 of D_2CO, a search for a rotational state dependence of lifetimes was carried out as follows. The shot-to-shot fluorescence from ~ 8×10^{-5} torr of D_2CO was observed as the fluorescence excitation spectrum was scanned over two spectral regions. The single shot S/N on an absorption peak was typically about five. The first region, from 27375 - 27394 cm^{-1}, includes mainly rR_1, rQ_2,

rR_2, rQ_3 lines, so that it samples $K' = 2 - 4$, and $J' = 3 - 15$. The second region, 27430 - 27440 cm^{-1}, includes rR_7 and rQ_9 lines and samples $K' = 8, 10$ and $J' = 8 - 19$. No variation of decay time was noticeable as the spectra were scanned. Any variation larger than a factor of two or three would have been observed. Signal-averaged decay curves were obtained at ten different fluorescence maxima. Single rotational states were typically not resolved in the $K' = 2 - 4$ region, since the D_2CO lines are very dense. The results are given in Table II. The decays were all single exponentials and the measured lifetimes ranged from 5.5 to 8.1 μs with a mean of 6.8 μs and a standard deviation of 1.0 μs. At 8×10^{-5} torr, a 7 μs lifetime is almost certainly collisionless to better than 10%.

D. Non-exponential decays.

In about 10% of the cases of seemingly clean excitation of H_2CO, the decay of total fluorescence was distinctly non-exponential. In all such cases, the decay was fit to a sum of two exponential components. The results are given in Table III, which includes the fast and slow lifetimes (τ_f and τ_s) and the t = 0 amplitude ratios I_f/I_s. The fast component always dominates the t = 0 amplitude. However, the slow component amplitudes are much too large to be rationalized as longer-lived fluorescence from states populated by collisions, even based on a relaxation rate as large as 200 μs^{-1} $torr^{-1}$.

The occurrence of such non-exponential decays is not evenly distributed across the spectrum. Note that $K' = 5$ and 7 contribute the bulk of the examples. These regions of the spectrum are not particularly crowded, and the lines are quite strong. On the other hand, the rP_0 and rQ_2 lines are weak and are found in crowded regions of the spectrum where unassigned lines are common. It is possible that the $rQ_2(3)$ and $rQ_2(4)$ results are non-exponential because both K-doublet components are excited, yet they have different lifetimes. If this were the case, one would expect $I_f/I_s = 1$, however. (See Table III for the relevant splittings, and see Section IV for further discussion).

Some of the τ_f results in Table III are shorter than those typical of the fast single exponential results of Table I. In particular, note τ_f for $rR_4(11)$ and $rQ_4(12)$, both of which terminate on $J' = 12$, $K' = 5$. The fast components are not quite obscured by the scattered light, and the two values of 30 nsec and 25 nsec are in good agreement. There is other, less direct evidence that a few states may have lifetimes less than 50 ns. The transitions $rR_0(1)$, $rR_0(3)$, $rQ_0(1)$, and $rQ_0(3)$ appear as minor peaks in the 4 torr fluorescence excitation spectrum. Yet no fluorescence was observed for these lines at pressures of a few mtorr. The relative intensities in the spectrum indicate that the low pressure fluorescence should be weak, but certainly observable. This suggests the possibility of a few very fast decays which are hidden by the scattered light pulse. The phenomenon was observed only in the four cases mentioned, so it is apparently uncommon.

IV. DISCUSSION

A. Previous results.

The tremendous variation of H_2CO decay rate with rotational state appears rather unique. For S_1 naphthalene, Schlag and co-workers have observed about a factor of two variation in both lifetime and fluorescence quantum yield as the excitation wavelength is scanned across the rotational contour of several single vibronic levels. Single rotational state resolution was not possible. In the case of S_1 glyoxal, Rordorf, et al.[5] found that ϕ_f varied less than 30% (the experimental uncertainty) for five $J'K'$ levels of the vibrationless state, in spite of the apparently unimolecular photochemical decay of glyoxal at the sub-mtorr pressures studied. Similarly, Parmenter and Schuh[12] found no dependence of the benzene $S_1 \rightarrow T_1$ intersystem crossing rate with rotational distribution, but rotational relaxation may have been important at the pressures studied.[6]

Several previous formaldehyde studies have indicated rotational state dependences of non-radiative rates in S_1 H_2CO. Tang, Fairchild and Lee[8] reported a factor of four variation in relative fluorescence quantum yield for single rotational levels of the $2^3 4^1$ level at 0.2 torr. No variation of ϕ_f was observed for the triplet-perturbed[8] $2^2 4^1$ level. The dependence within $2^3 4^1$ was attributed to Coriolis coupling with one of the <u>lower</u> levels $2^1 3^2 4^2$ or

$2^1 4^2 6^2$, which must be assumed to have a faster non-radiative rate than $2^3 4^1$. Coriolis coupling is not possible for the vibrationless level, and it is tempting to assume that the 4^0 mechanism operates for higher levels as well. More recently, Shibuya and Lee[11] have observed a factor of eight variation of ϕ_f with rotational state within 4^1 of H_2CO at 0.04 torr. Assuming a radiative lifetime of 3 μs for 4^1, the average observed ϕ_f of 0.031 corresponds to an average lifetime of 93 ns, somewhat shorter than the typical lifetimes of 160 ns reported here for 4^0. The 4^1 ϕ_f values are apparently not collisionless, since rotational relaxation at ~ 100 μs^{-1} $torr^{-1}$ competes with the non-radiative decay at 0.04 torr. Relaxation to more rapidly decaying levels causes the apparent ϕ_f to be less than the true collisionless value and obscures any long-lived states entirely.

Luntz[9] has measured fluorescence lifetimes of H_2CO in an effusive beam after excitation of 4_1^0 rR sub-band heads with 1.4 cm^{-1} resolution, so that several rotational levels are simultaneously excited. The time resolution of 100 nsec per channel resulted in preferential selection of long-lived states. The present work indicates that such states are quite unusual. In all cases ($K' = 1, 3, 5$), there is reasonable agreement between Luntz's lifetime and a higher resolution lifetime at excitation energies within 2 cm^{-1} of the rR head. Table IV gives a detailed comparison. The agreement is taken as confirmation of the claim that the present results are truly collisionless results.

Weisshaar, et al.[10] have also measured the fluorescence decay of 4^0_1 after excitation of rR sub-band heads with 1.5 cm^{-1} resolution. The decays were non-exponential except for $K' = 7$, and the fast and slow decay rates varied with K'. The lifetimes were much shorter than those of Luntz,[9] since there was no particular incentive to tune the laser to long-lived states. The present results clearly show that the non-exponential decays were due to direct laser excitation of several levels having different lifetimes. For $K' = 7$, the decay probably appeared exponential because the states populated had similar lifetimes.

The presently measured quenching rates of ~ 100 μsec^{-1} $torr^{-1}$ for H_2CO are quite comparable to the previously reported rates for faster states excited with 1.5 cm^{-1} resolution.[10] Given the wide variation of lifetime within 4^0, it is difficult to distinguish electronic quenching out of S_1 from rotational relaxation to states of much shorter lifetime than that initially excited. At pressures for which rotational equilibration is incomplete on the time-scale of the fastest decay rates, a significant fraction of the excited state molecules may decay via a few short-lived states, leading to a rapid apparent decrease of both τ and ϕ_f with increasing pressure. Simple kinetic models may be quite misleading in such a complicated situation.

For D_2CO, Luntz[9] obtained a 4^0_1 "bulb" lifetime of

7.4 ± 0.5 μs at each rR head for $K' = 2 - 12$. The presently measured 4^0_1 lifetimes were in the range 5.5 - 8.1 μs, in substantial agreement with Luntz. For 4^1 D_2CO, Shibuya and Lee[11] report a ± 29% variation (one standard deviation) of fluorescence quantum yields with rotational state at 5 mtorr, again suggesting a modest rotational state dependence of D_2CO lifetimes near the S_1 origin.

B. Zero pressure photophysics

The longest H_2CO zero pressure lifetime observed, 4.17 ± 0.20 μs for $J' = 4$, $K' = 1$, (--), is quite comparable to the S_1 pure radiative lifetime expected from theoretical calculations[21] and to the value of 3.3 μs derived from high pressure lifetimes and quantum yields for the 4^0 level by Lee and co-workers.[22, 23] There is no evidence for considerable lifetime lengthening[24] in either the lifetimes reported here or in the S_1 absorption spectrum, which appears sharp and essentially unperturbed. In the vast majority of the cases, the H_2CO zero pressure decay rates (Table I) are dominated by a fast non-radiative component. In contrast, the D_2CO zero pressure lifetimes (Table II) apparently vary only ± 20% about a typical value of 7 μs. These appear to be essentially radiative lifetimes. The slight variation might be due to a small non-radiative decay component. The isotope effect on τ_{rad} for a transition induced by the out of plane bend of the hydrogens (ν_4) is expected to be about a factor of two.

Sequential decay mechanism. The zero pressure non-radiative decay mechanism of low-lying S_1 levels of H_2CO is not well understood. The density of S_0 harmonic oscillator states near the S_1 origin is only 6 per cm^{-1}, and nearby T_1 levels are separated by tens of cm^{-1}. Thus, in the absence of collisions, H_2CO would appear to be a small molecule which should only radiate. However, the rapid, collisionless decay of most rotational states of S_1, 4^0 indicates the availability of some sort of continuum. The most plausible candidate at present is the H_2 + CO dissociative continuum. This requires either that the barrier between H_2CO (S_0) and H_2 + CO (whose height is not known) lie below the S_1 origin,[25] or that rapid quantum mechanical tunneling through the barrier be feasible. (See Sec. IV-C for further discussion). The mechanism assumed below thus involves indirect decay of S_1 to H_2 + CO via quasi-bound S_0 levels.

This sequential decay model is well-known in non-radiative transition theory.[2, 26] An initially prepared rotational state $|s\rangle$ of S_1 is coupled intramolecularly to a sparse set of bound S_0 levels $|\ell\rangle$, each of which is coupled in turn to the dissociative continuum of H_2 + CO levels, labeled $|m\rangle$. The coupling matrix elements are $V_{s\ell}$ and $V_{\ell m}$, respectively. Direct $|s\rangle$ to continuum couplings are ignored. Calculations[25] indicate that they are small, and the observed random variation of S_1 decay rate with J', K', and E_{rot} is inconsistent with a direct $S_1 \rightarrow H_2$ + CO mechanism. The zeroth order bound states have widths Γ_s and Γ_ℓ due to couplings to the various radiative or dissociative continua. This model has been solved in various ways,[1, 26] and the time evolution of the initial state $|s\rangle$ is quite complicated in general. However, in the "weak coupling limit" of $|V_{s\ell}| << |E_s - E_\ell + i(\Gamma_s - \Gamma_\ell)/2|$ for all ℓ, and under the assumption $\Gamma_\ell >> \Gamma_s$ for all ℓ, the non-radiative decay of $|s\rangle$ is exponential with a rate given by[26]

$$\Gamma_s^{nr} = (1/\hbar) \sum_\ell |V_{s\ell}|^2 \, \Gamma_\ell/[(\tilde{E}_s - \tilde{E}_\ell)^2 + (\Gamma_\ell/2)^2], \qquad (1)$$

where $\tilde{E}_s$ and $\tilde{E}_\ell$ are zeroth order energies corrected for level shifts.[26] The observation of single exponential decays suggests that if a sequential mechanism is correct, then the weak coupling limit is appropriate to formaldehyde. Calculations of the S_1 - S_0 matrix elements of the nuclear kinetic energy[25, 27] support such a model.

Within this framework, various possible explanations for the fluctuations of Γ_s^{nr} with J', K' and E_{rot} can be examined. As noted above, Coriolis coupling within S_1 cannot affect the vibrationless levels. The apparent lack of consistent trends with J' and K' argues against a strong rotational dependence of the intramolecular coupling $V_{s\ell}$. The data do indicate that, <u>on the average</u>, Γ_s^{nr} increases modestly with K' (or E_{rot}). The density of S_1 vibrational states increases only about 20% as E_{rot} increases from 0 to 1000 cm^{-1}, suggesting that the effect should be considered a K-dependence. Novak, et al.[28] have demonstrated an explicit K^2 dependence in the S_1 - S_0 matrix elements of the nuclear kinetic energy in a basis of Born-Oppenheimer <u>rovibronic</u> states due to an inter-electronic state Coriolis coupling. The effect is small compared with the usual vibronic coupling. A rotational state dependence of S_0 - continuum matrix elements (which determine the Γ_ℓ) is possible also.[28]

The primarily random variation of the decay rates can be understood in terms of Eq. (1). Conservation of J and perhaps K in the zero pressure non-radiative process[29] will limit the set of S_0 rotational states with which each S_1 state can interact. For each $J'K'$ state, the more nearly resonant the appropriate S_0 levels happen to be the stronger the intramolecular mixing will be, even if all the S_1 - S_0 coupling matrix elements were equal. The initial and final state rotational energies E_{rot} will be different in general. This causes different $J'K'$ states to interact strongly with different S_0 vibrational states, since the change in E_{rot} must be taken up by vibrational energy in S_0. Any variation in coupling matrix elements thus contributes directly to the variation in decay rate.[29]

Couplings. The usual vibronic couplings $\sum_k \partial^2/\partial Q_k{}^2$ are expected to dominate the intramolecular S_1 - S_0 perturbations $V_{s\ell}$, although much smaller, inter-electronic Coriolis couplings depending on K are present.[28] Only rovibronic states of the same species under the full symmetry group of the Hamiltonian can perturb each other. (See Section IIIA). Vibronic and D_2 (rotational sub-group) selection rules[29] are not rigorous, but they are correct to the extent that vibronic coupling dominates $V_{s\ell}$.

The total angular momentum J is conserved in the non-radiative process, restricting the number of S_0 rotational states which can couple to a given $J'K'$ state. However, more than one rotational state per S_0 vibrational state will interact with each $J'K'$ state because K is not a good quantum number. The asymmetric top, rigid rotor wavefunctions can be expanded in a symmetry-adapted symmetric top basis:[30]

$$|JK\pm\rangle = \sum_{K'} a_{JK'} \left(|JK'\rangle \pm |J\,-K'\rangle\right), \tag{2}$$

where the parity of K gives the C_2^a symmetry and the sign (±) gives the C_2^c symmetry. (See Section IIIA). The sum is restricted to K' even or odd according to whether K is even or odd. First-order perturbation theory shows that even for so nearly a symmetric top as formaldehyde, more than one $a_{JK'}$ is larger than 0.1 when J is larger than K + 3 or so. Consequently, the vibronic coupling connects more than one $|J''K''\pm\rangle$ with each $|J'K'\pm\rangle$ even though the selection rule is $\Delta K = 0$ in a symmetric top basis. Strong Coriolis coupling of nearly degenerate, high energy rovibronic levels of S_0 will further degrade K'' as a quantum number. A second-order x- or y-axis coupling mixes states of $\Delta K = \pm 1$; higher order couplings may be quite important when many states of appropriate symmetry are available within a few cm^{-1}.

Such considerations could dilute the vibronic coupling among as many as $(2J' + 1)$ rotational states per S_0 vibrational state. Except for resonance effects, the decay rate Γ_s^{nr} (Eq. 1) is unaffected, because the dilution of $|V_{s\ell}|^2$ cancels the increase in the number of $|\ell\rangle$ states contributing. Such effects would hasten the onset of a statistical limit in a larger molecule, since for N mutually perturbed S_0 levels the ratio V/ε is proportional to $\sqrt{N}$, where V is an average (diluted) matrix element and ε is a typical spacing between coupled levels.

<u>K-doublet behavior</u>. For each $J'K'$, the rigid rotor K-doublet splitting Δ can be computed accurately from the formula of Wang.[31, 32] The calculated S_1 splittings are given in Table V. Corresponding S_0 splittings are larger by a factor $(1.08)^K$. The lifetime behavior of the two doublet components changes qualitatively as the S_1 splitting Δ decreases below about 5×10^{-4} cm^{-1}. For $K' = 3$, $J' = 6$ ($\Delta = 8.1 \times 10^{-4}$ cm^{-1}), the (+-) and (--) decay rates differ by a factor of three. In all eight cases of larger Δ for which both lifetimes were measured (Table I), the decay rates are significantly different. In contrast, for $K' = 4$, $J' = 10$ ($\Delta = 1.7 \times 10^{-4}$ cm^{-1}), the two decay rates are apparently equal, since the $rR_3(9)$ transition populates both (++) and (-+) components yet the decay is a single exponential. Single exponential decays nearly always occur for $\Delta < 10^{-4}$ cm^{-1}, although both components are excited equally.

For every K-doublet pair, each state belongs to a different species of the full symmetry group, so that each interacts with its own set of S_0 states. If the perturbation is vibronic, then the D_2 symmetry will be conserved and Eq. (2) shows that the pair $|J'K' \pm\rangle$ will have identical sets of matrix elements $V_{s\ell}$ with the appropriate set of S_0 levels. Equation (2) further shows that (smaller) perturbations allowing $\Delta K = \pm 1, \pm 2$, etc. will also give the same set of matrix elements for $|J'K'+\rangle$ and $|J'K'-\rangle$ to first order, if $\Delta K < K$. Hence, it is a good assumption that each level of a K-doublet couples to its own set of S_0 levels, but that corresponding $V_{s\ell}$'s are the same.

There are then two possible explanations for the observed coalescence of the two lifetimes for $\Delta < 10^{-4}$ cm^{-1}. A small piece of the Hamiltonian may thoroughly mix the two doublets when they are so nearly degenerate, causing the lifetimes to become indistinguishable. Electronic-vibration-rotation interactions can be rigorously ruled out by symmetry. (Sec. IIIA). Nuclear spin-molecular rotation couplings are apparently much too small; in the ground electronic state of H_2CO they are less than 1 kHz.[33] Alternatively, the S_0 doublets coupled to S_1 may have become sufficiently degenerate so that each of the S_1 doublets sees essentially the same S_0 level structure.

Apparently for $\Delta \gtrsim 5 \times 10^{-4}$ cm^{-1}, the two S_1 doublets levels are not strongly mixed and see considerably different S_0 level structures. This implies that either the S_1 doublets or some of the important S_0 doublets have splittings comparable to typical S_0 spacings. (See Eq. 1). If K is a fairly good quantum number in S_0, this suggests a zero pressure density of coupled levels of 10^3 - 10^4 per cm^{-1}. On the other hand, if K is a poor quantum number in S_0 (as argued above), then $K' = 3$ would interact strongly with $K'' = 2$, whose doublet splitting is considerably larger (Table V). In either event, the suggestion is that the density of interacting states is larger than the harmonic oscillator level density of 10 per cm^{-1}. If it <u>were</u> as large as 10^3 - 10^4 per cm^{-1}, formaldehyde might be approaching a statistical limit, depending on typical $V_{s\ell}$ and Γ_ℓ values. A test of the level density might come from studies of the electric field dependence of the fluorescence decay. A Stark field will shift S_1 and S_0 levels relative to each other because the S_0 dipole moment is larger. The smallest field required to significantly affect the decay rate would indicate how large a relative energy shift is important.

C. Photochemistry

It must be emphasized that the sequential decay mechanism relies on the accessibility of the H_2 + CO dissociative continuum at zero pressure. The calculations of Heller, et al.[25] indicate that S_1 can indeed decay with a several hundred ns lifetime *if* the barrier to dissociation on S_0 lies *below* the S_1 origin. The calculated appearance of H_2 + CO is then rather prompt. D_2CO merely radiates because its S_1 - S_0

couplings are much smaller, essentially due to poorer vibrational overlaps. This may also explain the small D_2CO photochemical quantum yield at high pressures near the S_1 origin. If the barrier is above S_1, then Heller, et al., conclude that H_2CO and D_2CO are small molecules that should decay radiatively. It is conceivable that S_1 H_2CO is slightly above its effective barrier while D_2CO is below, due to different zero point energy changes. Quantum mechanical tunneling through the barrier may be quite rapid, as discussed below. It is of interest to learn whether or not D_2CO single rotational level decay rates begin to fluctuate strongly at energies similar to the threshold for D_2 + CO photochemistry.[34] The fate of S_1 molecules at zero pressure is not known; submtorr photochemistry has not been demonstrated. Detection of H_2 or CO photofragments in a molecular beam or in a very low pressure gas would provide considerable evidence in favor of the sequential decay model.

At pressures above 0.1 torr for energies near the S_1 origin, Houston and Moore[35] and Zughul[36] have shown that a very different mechanism operates. CO appears much more slowly than S_1 decays, and product formation requires a collision, i.e., the appearance rate is linear in pressure and extrapolates to zero at zero pressure. The appearance rate is roughly independent of formaldehyde isotope, excess energy in S_1 (from 0 to 1500 cm^{-1}), and collision partner (formaldehyde, He, Ar, Xe, NO).[35, 36] Apparently the high pressure behavior can be reconciled with fairly prompt zero pressure photochemistry only if long range collisions take the S_1 molecule to an intermediate state which does not fluoresce and which requires a further collision to dissociate. Above 0.1 torr, the collisional channel must dominate the zero pressure photochemical channel. A rate of quenching to the intermediate of 200 μs^{-1} $torr^{-1}$ (about 20 times the gas kinetic rate) would obscure an average zero pressure decay rate of 6 μs^{-1} at pressures above 0.1 torr. It is significant that such large quenching rates have in fact been observed.[10] The identity of the intermediate state remains unknown, although non-dissociative S_0 or T_1 levels[35] and the isomer HCOH[35, 37] have been mentioned as candidates. Ab initio calculations place the barriers to H_2 + CO and to HCOH above the S_1 origin by a few kcal/mole.[38, 39] Miller[40] has calculated collisionless $S_0 \rightarrow H_2$ + CO tunneling rates in a one-dimensional RRKM treatment at a given total energy using the barrier height and vibrational frequencies of Goddard and Schaefer.[39] He obtains a rate of 6×10^6 s^{-1} at the energy of the S_1 origin, strongly suggesting that S_0 can decay rapidly to molecular products even at energies 5 - 10 kcal/mole below the barrier. S_0 D_2CO is calculated to dissociate about 40 times slower.

V. CONCLUSION

The extreme variation of H_2CO zero pressure non-radiative decay rates with rotational state in 4^0 of S_1 has been well documented. No systematic quantum number dependence of the rates is observed. The results can be qualitatively understood in terms of a sequential decay through S_0 to H_2 + CO products, so that fluctuations in decay rate are largely due to resonance effects. The behavior of closely spaced K-doublets suggests the possibility of a high density of S_0 levels interacting with S_1 at zero pressure. It remains difficult to reconcile the fast, collisionless decay of S_1 with the delayed appearance of CO at higher pressures. The D_2CO zero pressure decay is dominated by the radiative rate.

ACKNOWLEDGMENTS

We thank the Division of Advanced Systems Materials Production, Office of Advanced Isotope Separation, U.S. Department of Energy under contract No. W-7405-Eng-48 and the National Science Foundation for their research support. We are grateful to K.F. Freed, M.L. Elert, W.M. Gelbart, D.F. Heller, J. Goddard, H.F. Schaefer III, R. Naaman, E.K.C. Lee, A.C. Luntz, and W.D. Gwinn for very useful discussion and for preprints of their work. J.C.W. thanks the National Science Foundation for a pre-doctoral fellowship.

REFERENCES

1. For a comprehensive review of theoretical and experimental work, see P. Avouris, W.M. Gelbart and M.A. El-Sayed, Chem. Rev. 77, 794 (1977).
2. K.F. Freed, Top. Appl. Phys. 15, 1 (1976); J.J. Jortner and S. Mukamel in "The World of Quantum Chemistry," R. Daudel and B. Pullman, Ed. (Reidel, Boston), 1974.
3. D.H. Levy, L. Wharton, and R.E. Smalley in "Chemical and Biochemical Applications of Lasers", Vol. II, C.B. Moore, Ed. (Academic Press, New York), 1977; J. Chaiken, T. Benson, and J.D. McDonald, to be published; F.M. Behlen, N. Mikami, and S.A. Rice, to be published.
4. R.A. Beyer, P.F. Zittel, and W.C. Lineberger, J. Chem. Phys. 62, 4016 (1975).
5. B.F. Rordorf, A.E.W. Knight, and C.S. Parmenter, Chem. Phys. 27, 11 (1978).
6. R.A. Coveleskie and C.S. Parmenter, J. Chem. Phys. 69, 1044 (1978).
7. U. Boesl, H.J. Neusser, and E.W. Schlag, Chem. Phys. Lett. 31, 1, 1975; W.E. Howard and E.W. Schlag, Chem. Phys. 17, 123 (1976).
8. K.Y. Tang, P.W. Fairchild, and E.K.C. Lee, J. Chem. Phys. 66, 3303 (1977).
9. A.C. Luntz, J. Chem. Phys. 69, 3436 (1978).
10. J.C. Weisshaar, A.P. Baronavski, A. Cabello, and C.B. Moore, J. Chem. Phys. 69, 4720 (1978).

11. K. Shibuya and E.K.C. Lee, J. Chem. Phys. 69, 5558 (1978).

12. C.S. Parmenter and M.D. Schuh, Chem. Phys. Lett. 13, 120 (1972).

13. V. Sethuraman, V.A. Job, and K.K. Innes, J. Mol. Spect. 33, 189 (1970).

14. B.J. Orr, Spectrochim. Acta 30A, 1275 (1974).

15. See footnote (i) under Table I.

16. D.C. Moule and A.D. Walsh, Chem. Rev. 75, 67 (1974).

17. G. Herzberg, "Electronic Spectra and Electronic Structure of Polyatomic Molecules," pp. 109 - 113, (Van Nostrand Reinhold), 1966.

18. H.C. Allen and P.C. Cross, "Molecular Vib-Rotors," p. 28, (John Wiley), 1963.

19. R.S. Mulliken, Phys. Rev. 59, 873 (1941); J.T. Hougen, J. Chem. Phys. 37, 1433 (1962); J.T. Hougen, ibid 39, 358 (1963).

20. (a) C.H. Townes and A.L. Schawlow, "Microwave Spectroscopy," (McGraw-Hill), 1955; (b) N. Jannuzzi and S.P.S. Porto, J. Mol. Spectrosc. 4, 459 (1960).

21. J.A. Pople and J.W. Sidman, J. Chem. Phys. 27, 1270 (1957); E.R. Farnworth, G.W. King, and D.C. Moule, Chem. Phys. 1, 82 (1973); M.J.H. Kemper, J.M.F. van Dijk, and H.M. Buck, to be published.

22. R.G. Miller and E.K.C. Lee, Chem. Phys. Lett. 33, 104 (1975); R.G. Miller and E.K.C. Lee, ibid 41, 52 (1976); R.G. Miller and E.K.C. Lee, J. Chem. Phys. 68, 4448 (1978).

23. K. Shibuya, R.A. Harger, and E.K.C. Lee, J. Chem. Phys. 69, 751 (1978).

24. A.E. Douglas, J. Chem. Phys. 45, 1007 (1966).

25. D.F. Heller, M.L. Elert, and W.M. Gelbart, J. Chem. Phys. 69, 4061 (1978).

26. A. Nitzan, J. Jortner, and P.M. Rentzepis, Proc. Roy. Soc. London A, 327, 367 (1972); A. Nitzan and J. Jortner, Theor. Chim. Acta (Berlin) 29, 97 (1973).

27. J.M.F. van Dijk, M.J.H. Kemper, J.H.M. Kerp, and H.M. Buck, J. Chem. Phys. 69, 2462 (1978).

28. F.A. Novak, S.A. Rice, and K.F. Freed, to be published.

29. W.E. Howard and E.W. Schlag, Chem. Phys. 29, 1 (1978); W.E. Howard and E.W. Schlag, J. Chem. Phys. 68, 2679 (1978).

30. H.W. Kroto, "Molecular Rotation Spectra," p. 45, (John Wiley), 1975.

31. C.H. Townes and A.L. Schawlow, "Microwave Spectroscopy," p. 87, (McGraw-Hill), 1955.

32. It can be shown that in the weak coupling limit (Eq. 1), level shifts do not seriously affect the S_1 splittings Δ, i.e., the perturbation of each doublet energy due to S_1 - S_0 interactions is small compared with the zeroth order spacing Δ.

33. P. Thaddeus, L.C. Krisher, and J.H.N. Loubser, J. Chem. Phys. 40, 257 (1964).

34. J.H. Clark, C.B. Moore, and N.S. Nogar, J. Chem. Phys. 68, 1264 (1978).

35. P.L. Houston and C.B. Moore, J. Chem. Phys. 65, 757 (1976).

36. M.B. Zughul, Ph.D. Dissertation, University of California, Berkeley, 1978.

37. J.R. Sodeau and E.K.C. Lee, Chem. Phys. Lett. 57, 71 (1978); M.J.H. Kemper, J.M.F. van Dijk, and H.M. Buck, J.A.C.S. 100, 7841 (1978).

38. R.L. Jaffee and K. Morokuma, J. Chem. Phys. 64, 4881 (1976).

39. J.D. Goddard and H.F. Schaefer III, J. Chem. Phys. submitted for publication.

40. W.H. Miller, J. Chem. Phys., submitted for publication.

TABLE I. H_2CO single exponential results for S_1 4^0.

Line[a]	ν_{vac}[a] (cm^{-1})	J'	K'[b]	C_2[c]	E_{rot}[c] (cm^{-1})	P_{min}[d] (mtorr)	τ(μs)[e]	τ^{-1}(μs^{-1})[e]
$rR_0(2)$	27034.0	3	1	-	20	0.5	3.55	0.282[f]
$rP_0(5)$	013.3	4	1	+	29	1.2	0.185	5.39
$rQ_0(4)$	026.6	4	1	-	30	0.4	4.17	0.240[f]
$rQ_0(5)$	025.5	5	1	+	41	0.9	0.298	3.36
$rQ_0(6)$	024.1	6	1	-	58	0.6	0.71	1.41[f]
$rQ_0(7)$	022.6	7	1	+	69	0.6	0.440	2.25[f]
$rQ_0(9)$	019.1	9	1	+	106	0.7	0.313	3.19
$rR_0(9)$	034.3	10	1	+	122	0.6	0.334	2.99
$rQ_0(11)$	014.9	11	1	+	152	0.7	0.528	1.89
$rR_0(10)$	033.2	11	1	-	144	0.7	0.298	3.35
$rR_0(11)$	031.8	12	1	+	169	0.3	0.64	1.55
$rQ_0(13)$	010.2	13	1	+	207	1.0	0.183	5.45
$rR_0(12)$	030.1	13	1	-	196	0.9	0.204	4.89
$rR_0(17)$	018.1	18	1	+	360	0.8	0.427	2.34
$rR_0(19)$	011.7	20	1	+	440	0.6	0.480	2.08
$rQ_2(6)$[g]	058.2	6	3	+	116	0.7	0.575	1.74
$rQ_2(6)$[g]	058.0	6	3	-	116	1.2	0.187	5.35
$rQ_2(7)$	055.9	7	3	+	131	1.2	0.168	5.96
$rQ_2(8)$	053.9	8	3	+	148	0.9	0.435	2.30
$rQ_2(8)$	053.4	8	3	-	148	1.7	0.085	11.7

TABLE I. H_2CO single exponential results. (continued)

Line[a]	ν_{vac}[a] (cm^{-1})	J'	K'[b]	C_2^c	E_{rot}[c] (cm^{-1})	P_{min}[d] (mtorr)	$\tau(\mu s)$[e]	$\tau^{-1}(\mu s^{-1})$[e]
$rQ_2(9)$	27050.6	9	3	+	167	1.2	0.198	5.04
$rQ_2(9)$	051.3	9	3	-	167	1.0	0.279	3.59
$rQ_2(10)$	048.5	10	3	+	188	1.2	0.245	4.07
$rQ_2(11)$	045.4	11	3	-	212	1.3	0.341	2.93
$rQ_2(12)$	042.1	12	3	+	237	0.7	0.76	1.31
$rQ_2(12)$	040.0	12	3	-	237	1.2	0.120	8.4
$rR_2(12)$	067.6	13	3	-	265	2.0	0.066	15.2
$rR_2(13)$	065.4	14	3	+	295	0.8	0.207	4.83[h]
$rQ_2(14)$	034.7	14	3	+	295	0.8	0.202	4.96[h]
$rR_2(13)$	068.4	14	3	-	295	1.1	0.69	1.45
$rR_2(14)$	066.8	15	3	+	327	1.1	0.364	2.74
$rQ_2(15)$	030.6	15	3	-	327	0.8	0.174	5.75
$rR_2(15)$	065.0	16	3	-	361	0.9	0.218	4.58
$rR_2(17)$	060.6	18	3	-	436	1.3	0.135	7.4
$rR_3(3)$	090.8	4	4	±	147	1.2	0.322	3.11[h]
$rQ_3(4)$	081.2	4	4	±	147	0.8	0.314	3.18[h]
$rQ_3(5)$	079.7	5	4	±	158	1.0	0.137	7.3
$rR_3(5)$	092.5	6	4	±	171	1.2	0.098	10.2
$rQ_3(7)$	075.9	7	4	±	186	1.6	0.190	5.25
$rQ_3(8)$	073.5	8	4	±	203	1.6	0.284	3.51
$rR_3(9)$	092.2	10	4	±	243	1.5	0.116	8.6
$rR_4(4)$	112.3	5	5	±	229	1.9	0.098	10.2
$rR_4(5)$	113.0	6	5	±	242	1.7	0.085	11.7

TABLE I. H_2CO single exponential results. (continued)

Line[a]	ν_{vac}[a] (cm^{-1})	J'	K'[b]	C_2^c	E_{rot}[c] (cm^{-1})	P_{min}[d] (mtorr)	$\tau(\mu s)$[e]	$\tau^{-1}(\mu s^{-1})$[e]
$rR_4(9)$	27112.7	10	5	±	314	1.7	0.113	8.8[h]
$rQ_4(10)$	088.5	10	5	±	314	1.5	0.109	9.2[h]
$rR_4(12)$	109.4	13	5	±	391	1.6	0.163	6.2
$rR_4(13)$	107.7	14	5	±	421	0.9	0.287	3.48[h]
$rQ_4(14)$	073.8	14	5	±	421	0.9	0.270	3.71[h]
$rR_4(15)$	103.4	16	5	±	487	1.8	0.242	4.14
$rR_4(16)$	100.8	17	5	±	523	1.4	0.236	4.24
$rR_5(8)$	133.9	9	6	±	380	2.0	0.123	8.2
$rR_5(10)$	132.5	11	6	±	424	2.5	0.068	14.8
$rR_5(11)$	131.3	12	6	±	450	1.5	0.167	5.99[h]
$rQ_5(12)$	102.2	12	6	±	450	2.2	0.170	5.90[h]
$rR_5(13)$	128.1	14	6	±	507	1.6	0.158	6.32
$rR_5(14)$	126.0	15	6	±	539	2.0	0.106	9.4
$rR_5(16)$	120.8	17	6	±	610	1.6	0.200	5.00
$rQ_6(7)$	137.8	7	7	±	446	1.0	0.137	7.3
$rR_6(8)$	154.5	9	7	±	482	0.7	0.200	5.00[h]
$rQ_6(9)$	132.7	9	7	±	482	1.4	0.187	5.34[h]
$rR_6(9)$	153.1	10	7	±	504	1.0	0.088	11.3
$rQ_6(11)$	126.5	11	7	±	527	2.9	0.079	12.6
$rR_6(11)$	151.9	12	7	±	553	1.1	0.156	6.4[h]
$rQ_6(12)$	122.9	12	7	±	553	1.8	0.160	6.3[h]
$rR_6(16)$	141.6	17	7	±	712	0.7	0.224	4.47
$rR_6(17)$	138.6	18	7	±	750	1.4	0.139	7.18

TABLE I. H_2CO single exponential results. (continued)

Line[a]	ν_{vac}[a] (cm^{-1})	J'	K'[b]	C_2^c	E_{rot}[c] (cm^{-1})	P_{min}[d] (mtorr)	$\tau(\mu s)$[e]	$\tau^{-1}(\mu s^{-1})$[e]
$rR_7(7)$	27175.1	8	8	±	581	1.3	0.136	7.37
$rR_7(8)$	174.8	9	8	±	601	1.7	0.179	5.58
$rR_7(9)$	174.3[i]	10	8	±	622	0.8	0.200	5.00
$rR_7(10)$	173.4[i]	11	8	±	645	1.0	0.244	4.09
$rR_7(11)$	172.2	12	8	±	671	1.5	0.111	9.0
$rR_7(12)$	170.8	13	8	±	698	1.7	0.109	9.2
$rR_7(13)$	169.0	14	8	±	728	1.8	0.113	8.85
$rR_7(16)$	161.8	17	8	±	830	1.9	0.123	8.13
$rR_8(8)$	194.7	9	9	±	735	0.6	0.452	2.21[h]
$rQ_8(9)$	172.9	9	9	±	735	0.9	0.444	2.25[h]
$rR_8(9)$	194.1	10	9	±	756	1.2	0.172	5.80[h]
$rQ_8(10)$	169.9	10	9	±	756	1.4	0.185	5.41[h]
$rR_8(10)$	193.2	11	9	±	779	1.0	0.200	5.00[h]
$rQ_8(11)$	166.6	11	9	±	779	1.5	0.192	5.20[h]
$rR_8(11)$	192.0	12	9	±	805	2.1	0.109	9.2[h]
$rQ_8(12)$	163.1	12	9	±	805	1.8	0.114	8.8[h]
$rR_8(12)$	190.6	13	9	±	833	1.7	0.109	9.2[h]
$rQ_8(13)$	159.2	13	9	±	833	1.7	0.118	8.5[h]
$rR_8(13)$	188.8	14	9	±	862	2.0	0.118	8.5
$rR_8(14)$	186.7	15	9	±	894	1.4	0.173	5.79
$rR_8(15)$	184.3	16	9	±	928	1.3	0.178	5.63[h]
$rQ_8(16)$	145.7	16	9	±	928	1.5	0.182	5.48[h]
$rR_8(16)$	181.6	17	9	±	965	1.4	0.213	4.69[h]

TABLE I. H_2CO single exponential results. (continued)

Line[a]	ν_{vac} [a] (cm^{-1})	J'	K'[b]	C_2^c	E_{rot} [c] (cm^{-1})	P_{min} [d] (mtorr)	$\tau(\mu s)$ [e]	$\tau^{-1}(\mu s^{-1})$ [e]
$rQ_8(17)$	27140.5	17	9	±	965	1.5	0.207	4.83[h]
$rR_8(17)$	178.6	18	9	±	1003	1.8	0.138	7.3
$rR_8(18)$	175.3	19	9	±	1043	1.4	0.187	5.34
$rR_8(19)$	171.7	20	9	±	1086	2.0	0.098	10.2
$rR_8(20)$	167.8	21	9	±	1131	2.3	0.086	11.6
$rR_8(21)$	163.5	22	9	±	1177	1.9	0.177	5.65
$rR_9(9)$	213.4	10	10	±	906	1.2	0.217	4.60
$rR_9(10)$	212.5	11	10	±	929	1.9	0.074	13.5
$rR_9(11)$	211.3	12	10	±	955	1.8	0.169	5.93
$rR_9(13)$	208.0	14	10	±	1012	2.0	0.238	4.20
$rR_{10}(10)$	231.1	11	11	±	1095	2.1	0.081	12.3
$rR_{10}(11)$	229.9	12	11	±	1120	1.9	0.104	9.6
$rR_{10}(12)$	228.4	13	11	±	1148	2.5	0.106	9.4
$rR_{10}(13)$	226.6	14	11	±	1178	2.0	0.128	7.8
$rR_{10}(14)$	224.5	15	11	±	1210	2.0	0.115	8.7

Footnotes for Table I.

[a] The assignments are those of Sethuraman, et al., Ref. (13). The transition frequency ν_{vac} has been rounded to the nearest 0.1 cm^{-1}. See Sec. III-A of the text for an explanation of the notation.

[b] The rotational symmetry species of the excited state under the D_2 rotational sub-group. See Sec. IIIA of the text. In the "(+-)" notation, the parity of K' gives the second label (even → +, odd → -) and the entry under C_2^c gives the first label. When "±" is entered, both doublet components were excited equally.

[c] The rigid rotor energies obtained by interpolation in Appendix IV of Ref. (20a) or in Table I of Ref. (20b).

[d] The minimum pressure studied, in mtorr. See Sec. IIIB of the text.

[e] Lifetimes and decay rates at the lowest pressure studied. Accuracy is ± 5% (± 2σ).

[f] These τ^{-1} were obtained by extrapolating a Stern-Volmer plot to zero pressure.

[g] The $rQ_2(6)$ doublets were only partially resolved. See Sec. IIIC of the text.

[h] These states were excited via two different transitions, so that the decay rates serve as cross-checks.

Footnotes for Table I. (continued)

[i] The $rR_7(9)$ and $rR_7(10)$ lines did not match the transition frequencies given in Ref. (13), which were 27174.6 and 27174.0 cm^{-1}, respectively. No lines appeared at those frequencies. The observed lines are strong, and all the observed frequencies fit a parabolic function of J' better than those of Ref. (13), suggesting that the assignment here is correct.

TABLE II. D_2CO lifetimes for S_1 4^0.

$\nu_{vac}(cm^{-1})$ [a]	$\tau(\mu s)$ [b]	Line(s) [a]	J'	K' [c]	C_2^c
27375.5	5.87	$rR_1(14)$	15	2	+
		$rQ_3(13)$	13	4	+
27376.8	7.6	$rR_1(13)$	14	2	-
27378.0	8.1	$rR_1(12)$	13	2	+
		$rQ_2(7)$	7	3	+
		$rQ_3(12)$	13	4	-
27379.7	5.81	$rQ_2(6)$	6	3	-
		$rQ_3(11)$	11	4	-
27380.9	7.5	$rR_1(3)$	4	2	-
		$rR_1(9)$	10	2	-
		$rQ_2(5)$	5	3	+
27383.7	6.6	$rR_1(4)$	5	2	-
27430.1	8.1	$rR_7(18)$	19	8	±
27431.6	6.2	$rR_9(13)$	14	10	±
27435.0	7.2	$rR_7(15)$	16	8	±
27438.1	5.54	$rR_7(12)$	13	8	±

Footnotes for Table II.

[a] The assignments are those of Orr, Ref. (14). The transition energy ν_{vac} has been rounded to the nearest 0.1 cm^{-1}.

[b] Lifetime at ~ 8 x 10^{-5} torr of D_2CO. Accuracy is ± 5% (± 2σ). These lifetimes are probably collisionless to better than 10%.

[c] See footnote (b) of Table I.

TABLE III. H_2CO non-exponential results.

Line[a]	ν_{vac}[a] (cm^{-1})	J'	K'	P_{min}[b] (mtorr)	τ_f(ns)[c]	τ_s(ns)[c]	I_f/I_s[c]
$rP_0(6)$	27009.2	5	1	1.0	210	~900	4
$rQ_2(3)$	062.5	3	3	1.6	50	~160	3
$rQ_2(4)$	061.3	4	3	1.0	330	1300	3
$rQ_4(7)$	096.4	7	5	1.3	70	290	4
$rQ_4(8)$	094.1	8	5	1.1	130	370	3
$rR_4(10)$	111.9	11	5	1.1	130	565	10
$rR_4(11)$	110.8	12	5	1.7	30	130	10
$rQ_4(12)$	081.8	12	5	2.0	25	~80	10
$rR_6(13)$	148.7	14	7	1.5	60	~150	3
$rR_6(14)$	146.6	15	7	1.5	50	~160	7
$rR_6(15)$	144.3	16	7	1.5	75	230	3

[a] See footnote (a) of Table I.

[b] See footnote (b) of Table I.

[c] The non-exponential decays were fit to a sum of a fast (τ_f) and a slow (τ_s) exponential decay in all cases. I_f/I_s is the t = 0 amplitude ratio, accurate to ± 30%. The uncertainties in τ_f and τ_s are ± 15% unless preceded by a "~" in which cases τ_s was weak and was determined only to ±50%.

TABLE IV. Comparison of high resolution H_2CO lifetimes with those of Luntz.

rR Head	Luntz' $\tau(\mu s)$[a]	This work Line[b]	ν_{vac}[b] (cm^{-1})	P_{min}[c] (mtorr)	$\tau(\mu s)$
$K' = 1$	3.6 ± 0.3	$rR_0(2)$	27034.0	0.5	3.55 ± 0.18[d]
$K' = 3$	2.6 ± 0.3	$rR_2(3)$ } $rR_2(11)$ }	27071.0	0.5	1.80 ± 0.09[e]
$K' = 5$	0.7 ± 0.3	$rR_4(10)$	27111.9	1.1	0.565 ± 0.028

[a] Taken from Ref. (9).

[b] See footnote (a) of Table I.

[c] See footnote (b) of Table I.

[d] Zero pressure extrapolation of 0.5 to 10 mtorr Stern-Volmer plot.

[e] The excitation is impure and the 1.8 μs decay is the slow component of a biexponential decay. A correction for the finite pressure would lengthen the zero pressure lifetime to about 2.0 μs.

TABLE V. Splitting of K-doublets[a] for 4^0 of S_1 H_2CO, Δ in cm^{-1}.

J'	K' = 1	K' = 2	K' = 3	K' = 4	K' = 5
3	0.72	6.8(-3)	9.7(-6)		
4	1.2	2.0(-2)	6.8(-5)	5.7(-8)	
5	1.8	4.8(-2)	2.7(-4)	5.1(-7)	3.0(-10)
6	2.5	9.5(-2)	8.1(-4)	2.6(-6)	3.3(-9)
7	3.3	0.17	2.0(-3)	9.4(-6)	2.0(-8)
8	4.3	0.29	4.5(-3)	2.8(-5)	8.7(-8)
9	5.4	0.45	8.9(-3)	7.3(-5)	3.0(-7)
10	6.5	0.67	1.7(-2)	1.7(-4)	9.1(-7)
11	7.8	0.97	2.9(-2)	3.7(-4)	2.4(-6)
12	9.3	1.36	4.8(-2)	7.3(-4)	5.9(-6)
13	10.8	1.86	7.7(-2)	1.4(-3)	1.3(-5)
14	12.4	2.48	0.12	2.5(-3)	2.8(-5)
15	14.1	3.24	0.18	4.3(-3)	5.6(-5)
20	24.1	9.95	0.92	0.12	9.9(-4)

[a] Computed from Wang's formula (Ref. 31):

$$\Delta = b^K (J + K)! \;/\; \{8^{K-1} \left[(K - 1)!\right]^2 (J - K)!\},$$ where

$b = (C - B)/(2A - B - C)$. Formula is accurate to a few percent for so nearly symmetric a top. Corresponding S_0 Δ's can be obtained by multiplying each entry by $(1.08)^K$.

Figure 1. A 10 cm^{-1} segment of the 2 torr fluorescence excitation spectrum of the 4^0_1 band of H_2CO. The apparent laser linewidth is about 0.15 cm^{-1} FWHM. The rotational symmetries are those of the upper level.

Figure 2. Decay of total fluorescence after 4^0_1 excitation of H_2CO to the $J' = 12$, $K' = 3$, (+-) and to the $J' = 10$, $K' = 5$ levels. Both K-doublets are excited in the latter case. The pressures are 0.7 mtorr and 1.5 mtorr, respectively. The lifetimes are 760 ns and 110 ns, respectively.

Figure 3. Distribution of decay rates over 1 μs^{-1} intervals for the 90 H_2CO rotational states for which a single exponential decay was observed (Table I).

Figure 4. Detailed plot of the H_2CO single exponential decay rates (Table I) vs J' for various K'. Individual K-doublet rates are shown whenever selective excitation was possible.

Figure 5. Plot of H_2CO decay rates averaged over J' for each K'. The vertical bars indicate the range of rates included in each average, while the numbers in parentheses indicate how many individual rates were included. There is a modest trend of increasing average rate with K'.

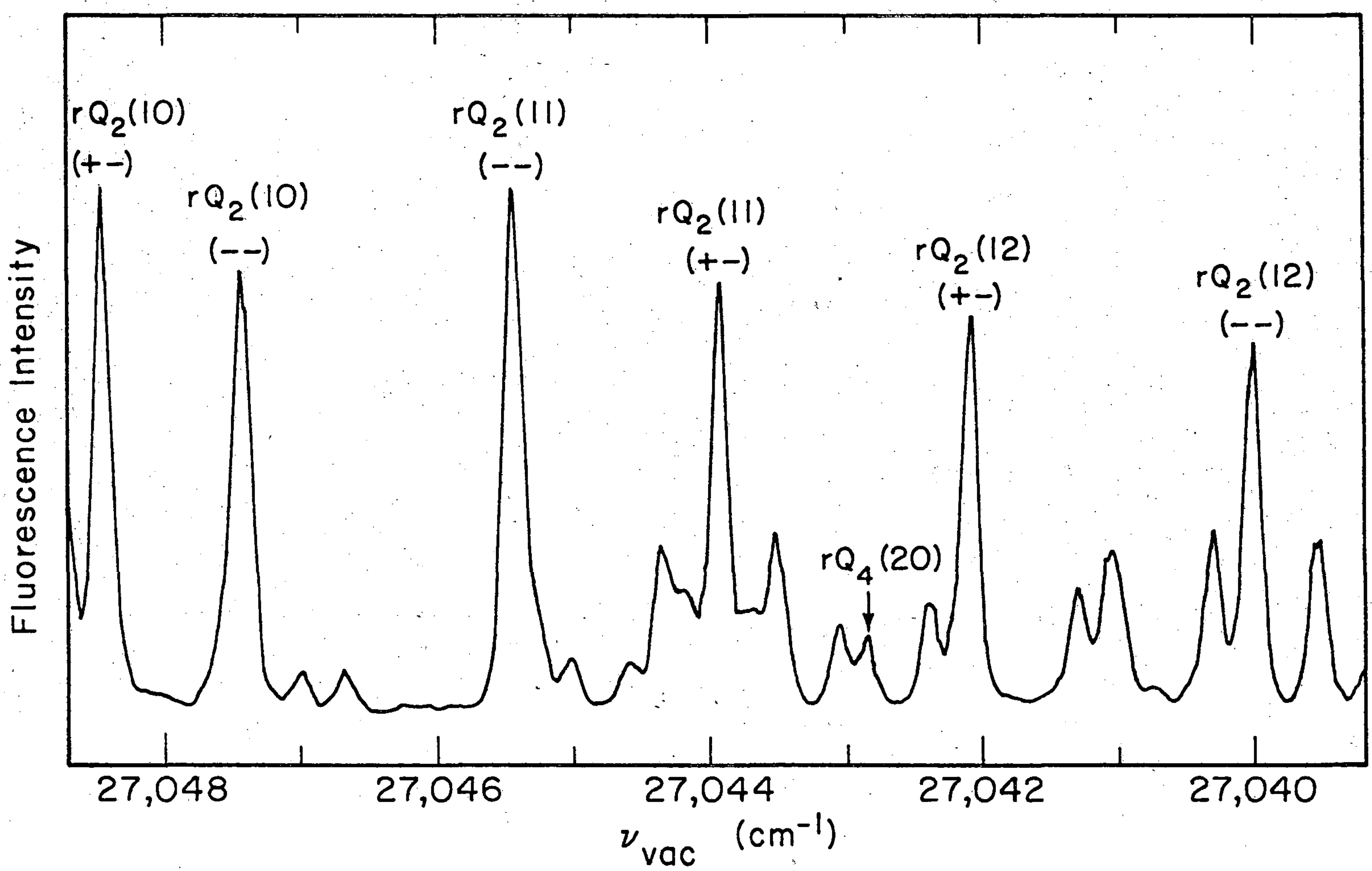

XBL 7812-13702

Fig. 1

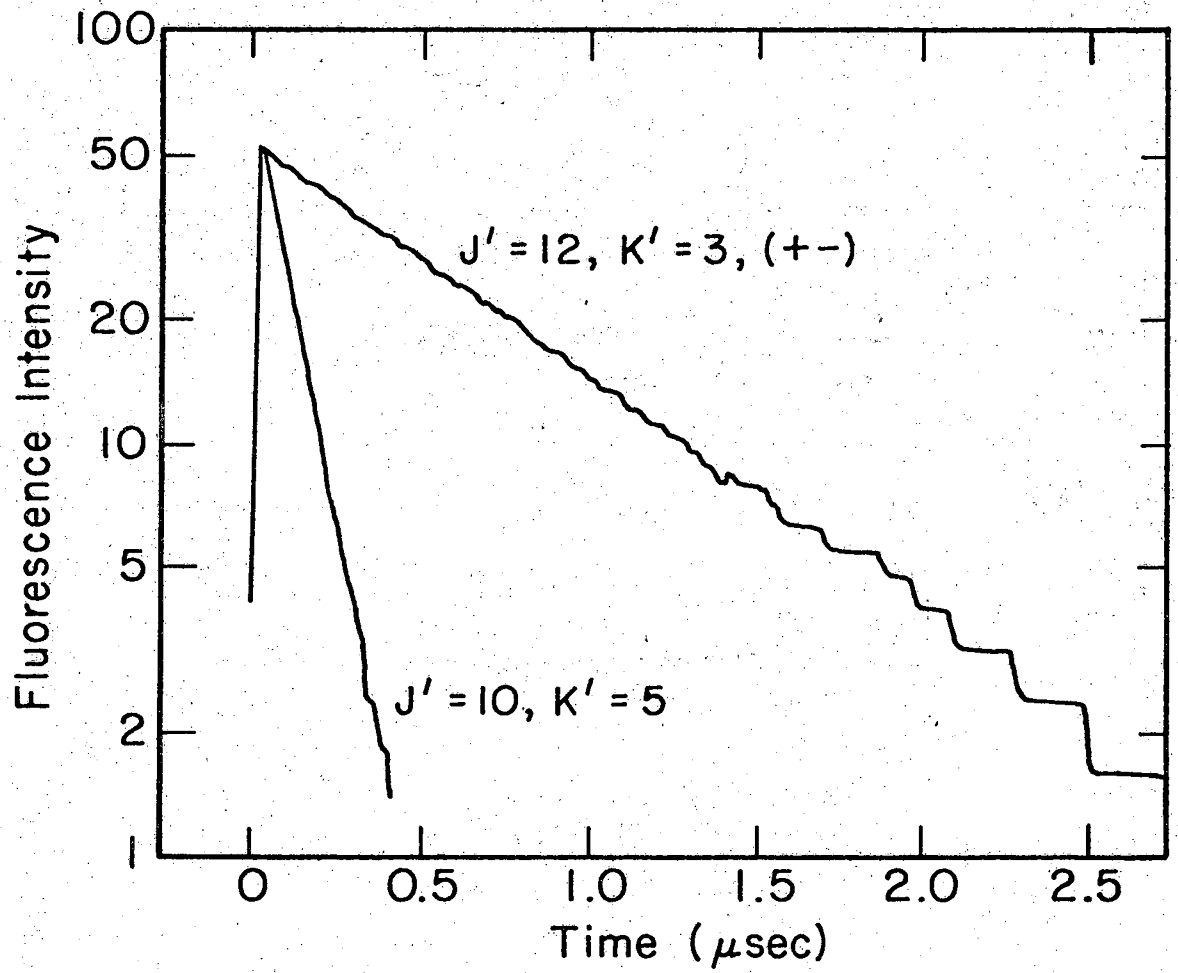

XBL 7812-13701

Fig. 2

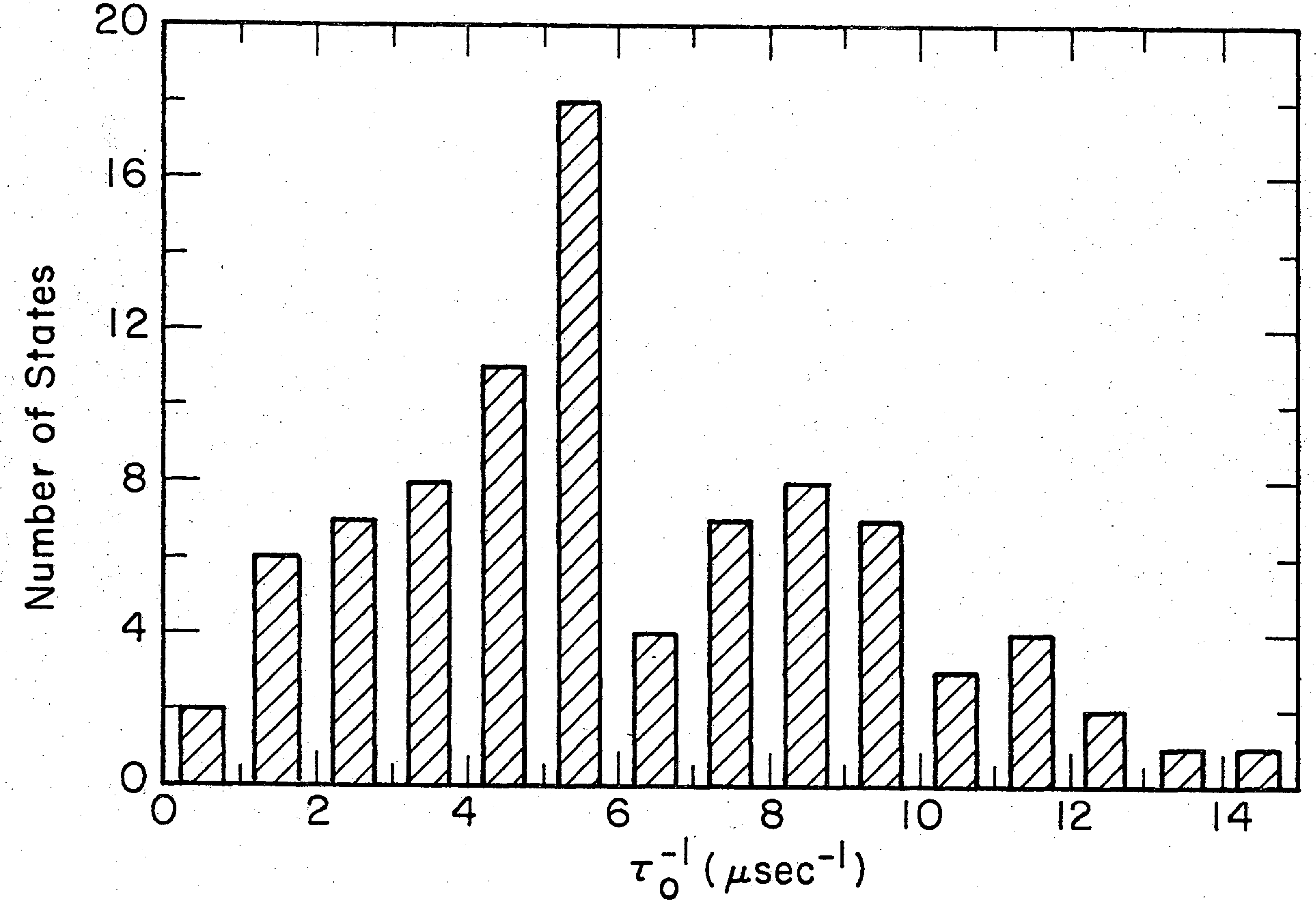

XBL 7812-13700

Fig. 3

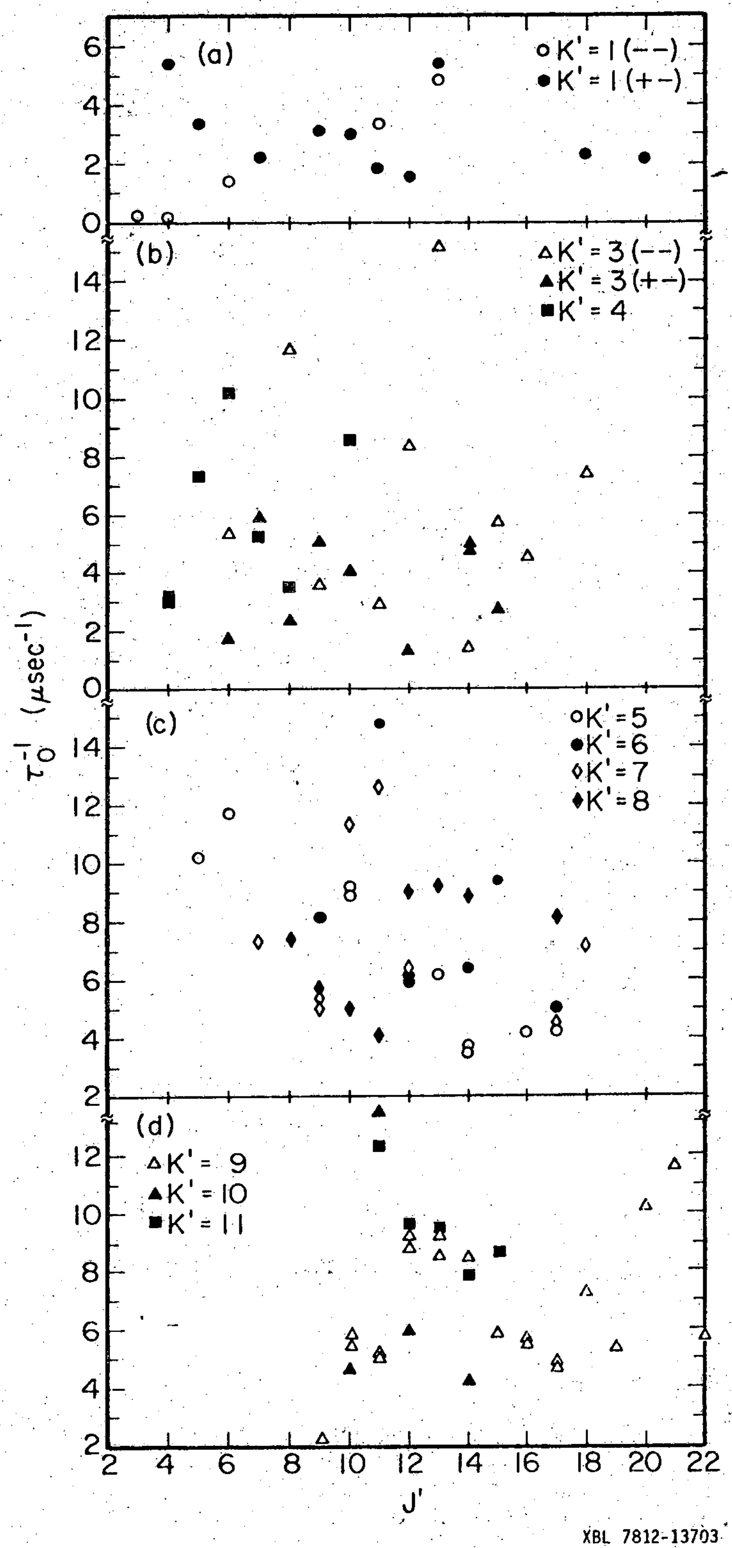
(a)
○ K' = 1 (− −)
● K' = 1 (+ −)
(b)
△ K' = 3 (− −)
▲ K' = 3 (+ −)
■ K' = 4
(c)
○ K' = 5
● K' = 6
◊ K' = 7
♦ K' = 8
(d)
△ K' = 9
▲ K' = 10
■ K' = 11
τ_0^{-1} (μsec^{-1})
J'
XBL 7812-13703

Fig. 4

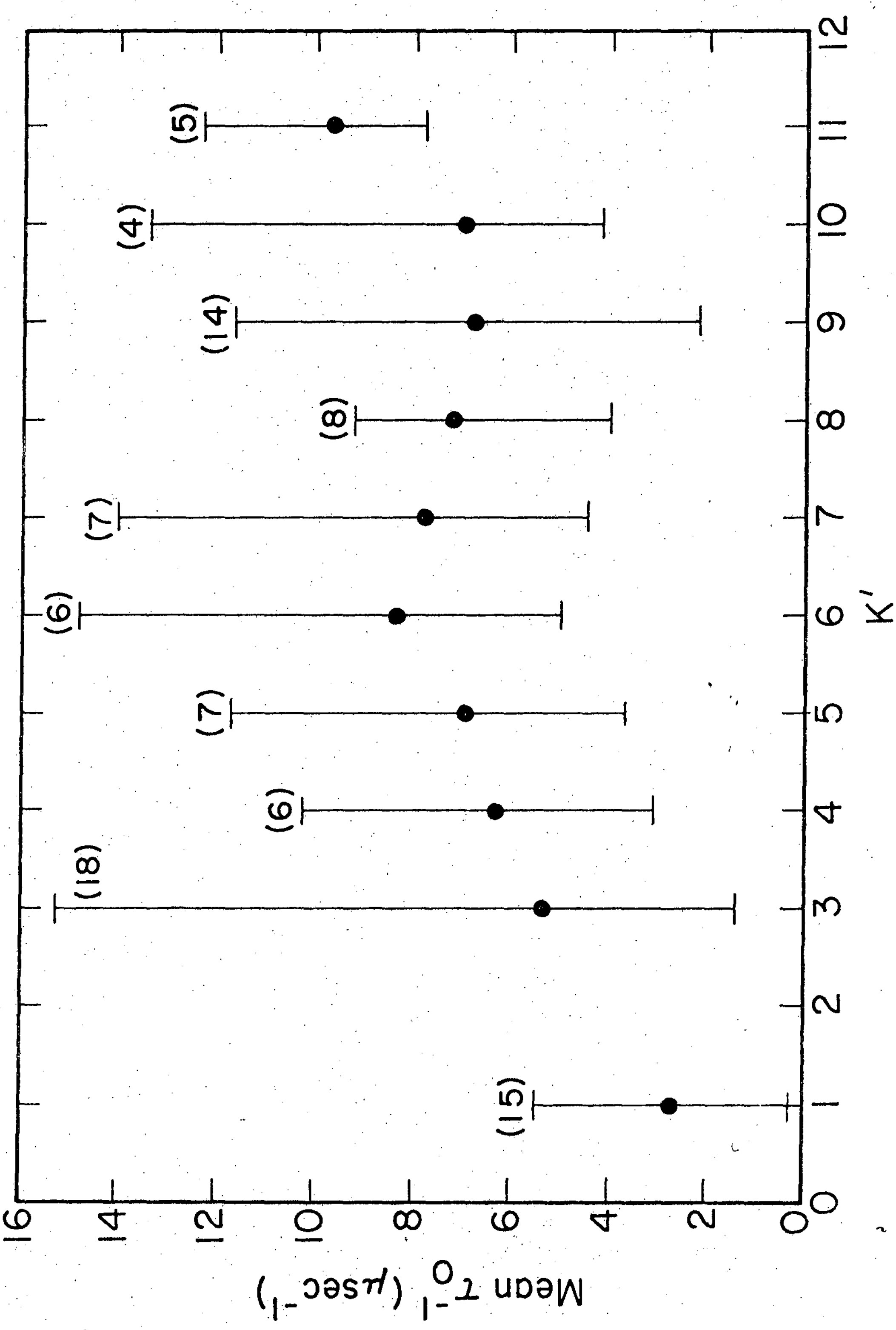

XBL 787-9608a

Fig. 5

TECHNICAL INFORMATION DEPARTMENT
LAWRENCE BERKELEY LABORATORY
UNIVERSITY OF CALIFORNIA
BERKELEY, CALIFORNIA 94720